Title: Transcriptional regulation by nicotine in dopaminergic neurons

Authors: Beverley M. Henley Brian A. Williams Rahul Srinivasan Bruce N. Cohen Cheng Xiao Elisha D.W. Mackey Barbara J. Wold Henry A. Lester

PII: S0006-2952(13)00483-8
DOI: http://dx.doi.org/doi:10.1016/j.bcp.2013.07.031
Reference: BCP 11718

To appear in: *BCP*

Received date: 8-5-2013
Revised date: 26-7-2013
Accepted date: 26-7-2013

Please cite this article as: Henley BM, Williams BA, Srinivasan R, Cohen BN, Xiao C, Mackey EDW, Wold BJ, Lester HA, Transcriptional regulation by nicotine in dopaminergic neurons, *Biochemical Pharmacology* (2013), http://dx.doi.org/10.1016/j.bcp.2013.07.031

Transcriptional regulation by nicotine in dopaminergic neurons

Beverley M. Henley, Brian A. Williams, Rahul Srinivasan, Bruce N. Cohen, Cheng Xiao, Elisha D.W. Mackey, Barbara J. Wold, Henry A. Lester

California Institute of Technology, 156-29 Caltech, Pasadena, CA 91125, USA.

Running Title Page:

RNA-Seq after chronic nicotine in identified neurons

Corresponding authors:

Henry A. Lester, email: lester@caltech.edu tel.: +1 626 395 4946, fax: +1 626 564 8709

Beverley M. Henley, email: bhenley@caltech.edu tel.: +1 626 395 6063, fax: +1 626 564 8709

California Institute of Technology, 156-29 Caltech, Pasadena, CA 91125, USA

Abbreviations

DAVID: Database for Annotation, Visualization and Integrated Discovery

ER: endoplasmic reticulum

FPKM: fragments per kilobase per million mapped reads

IPA: Ingenuity Pathway Analysis

nAChR: nicotinic acetylcholine receptor

PD: Parkinson's disease

SNc: substantia nigra pars compacta

UPR: unfolded protein response

VTA: ventral tegmental area

Document statistics

Main text: 20 pages

1 Graphical abstract (1 .ppt)

4 Figure files (4 .pptx)

4 Tables

1 Figure caption file

Abstract

Dopaminergic neurons in the substantia nigra pars compacta (SNc) degenerate in Parkinson's disease. These neurons robustly express several nicotinic acetylcholine receptor (nAChR) subtypes. Smoking appears to be neuroprotective for Parkinson's disease but the mechanism is unknown. To determine whether chronic nicotine-induced changes in gene expression contribute to the neuroprotective effects of smoking, we develop methods to measure the effect of prolonged nicotine exposure on the SNc neuronal transcriptome in an unbiased manner. Twenty neurons were collected using laser-capture microscopy and transcriptional changes were assessed using RNA deep sequencing. These results are the first whole-transcriptome analyses of chronic nicotinic treatment in SNc neurons. Overall, 129 genes were significantly regulated: 67 upregulated, 62 downregulated. Nicotine-induced relief of endoplasmic reticulum (ER) stress has been postulated as a potential mechanism for the neuroprotective effects of smoking. Chronic nicotine did not significantly affect the expression of ER stress-related genes, nor of dopamine-related or nAChR genes, but it did modulate expression of 129 genes that could be relevant to the neuroprotective effects of smoking, including genes involved in (1) the ubiquitin-proteasome pathway, (2) cell cycle regulation, (3) chromatin modification, and (4) DNA binding and RNA regulation. We also report preliminary transcriptome data for single-cell dopaminergic and GABAergic neurons isolated from midbrain cultures. These novel techniques will facilitate advances in understanding the mechanisms taking place at the cellular level and may have applications elsewhere in the fields of neuroscience and molecular biology. The results give an emerging picture of the role of nicotine on the SNc and on dopaminergic neurons.

Keywords:

Nicotinic acetylcholine receptor, RNA-Seq, Substantia nigra pars compacta, Dopamine-related genes, Ubiquitin-proteasome pathway

1. Introduction

Nicotine is the major addictive compound in tobacco, affecting ~20% of the world's population which in turn results in five million deaths worldwide each year [1]. Inhaled nicotine is efficiently delivered to the central nervous system where it affects various molecular and cellular processes [2, 3]. In the brain, nicotine selectively interacts with its central targets, the nicotinic acetylcholine receptors (nAChRs). The 12 nAChR subunits combine in a variety of stoichiometries to form pentameric ligand-gated cation channels. The multiple subtypes of nAChRs bind nicotine, but with a range of affinities. Nicotine binds to and activates some nAChR subtypes (high-sensitivity nAChRs) more than others nAChRs (low-sensitivity nAChRs), and can result in activation, then desensitization, of nAChRs. Another level of complexity of the actions of nicotine arises from the widespread and non-uniform distribution of nAChR subtypes throughout the brain [2]. Hence, nicotine influences many centrally regulated functions, in addition to the reward systems. In addition to the commonly reported changes in nicotinic acetylcholine receptors (nAChRs) [4-10], chronic nicotine exposure also leads to transcriptional changes throughout the brain [11-15]. Given the complexity of these interactions it is unsurprising that much remains to be learned about the effects, transcriptional and otherwise, of nicotine on the brain.

The substantia nigra pars compacta (SNc) dopaminergic neurons robustly express several nAChR receptor subtypes [16]. Nicotine exposure activates SNc nAChRs at the plasma membrane, increasing firing frequency and therefore resulting in release of dopamine in the dorsal striatum. The best-studied effect of chronic nicotine is the upregulation of the nicotinic receptor protein subunits themselves. Furthermore, following nicotine exposure, neuronal transcriptomes are altered [11-15]. However, the transcriptome-wide response to nicotine in the SNc is not clearly understood.

Parkinson's disease (PD) is currently an incurable, age-related neurodegenerative disorder. Although common, the etiology remains poorly understood [17, 18]. Familial causes of PD only account for 10% of PD cases, 90% of cases appear to be sporadic, however genetic susceptibility may play a role in sporadic PD. Several genes are associated with familial forms of PD and include: Pink1 (Park6), DJ-1 (Park 7), UCHL1 (Park 5; proteasomal protein), SNCA (Park 1,4), Park2 (Parkin; a ubiquitin E2 ligase) and LRRK2 [19]. In PD there is widespread neuronal loss throughout the brain with pronounced neuronal degeneration of DA neurons of the SNc. The death of DA neurons in the SNc contributes to the loss of dopamine in the striatum, a brain region involved in the control of movement, leading to diagnostic clinical features of bradykinesia, rigidity and tremor. Interestingly, a person's history of tobacco use is inversely correlated with his/her risk of Parkinson's disease (PD) [20, 21]. The protective effects of nicotine may be twofold: (1) nicotine exposure activates SNc nAChRs at the plasma membrane, increasing firing frequency and therefore increasing release of dopamine in the dorsal striatum, and (2) the distinct molecular pathways that are regulated by nicotine may exert neuroprotective effects. In addition to nicotine, smoked or smoke-cured tobacco releases numerous other components, any of which may play an additive role in protection against nigrostriatal damage [22]. This apparent neuroprotective effect of smoking has been modeled in animals, and the data show a strong protective effect of nicotine itself [23-27]. However, smoked or smoke-cured

tobacco will never be a medically acceptable therapy. Therefore it is important to understand the mechanism of apparent inadvertent neuroprotective and/or therapeutic effects of chronic exposure to nicotine. In this study we wanted to develop methods to determine whether chronic nicotine-induced changes in gene expression contribute to the neuroprotective effects of nicotine. Furthermore, there may be transcriptional modifications due to nicotine exposure in the SNc in the healthy brain, and we would like to obtain a clear understanding of this.

Here we investigate the effects of chronic nicotine treatment versus saline treatment on wildtype mouse SNc neurons. We collect and pool ~20 SNc neurons using laser-capture microscopy, then assess transcriptional modifications by deep sequencing. We give the first whole-transcriptome analysis of nicotinic treatment on SNc cells. Globally, we find that the expression levels of a total of 129 genes are significantly modulated, 67 are upregulated, and 62 are downregulated, by chronic nicotine exposure in our unbiased study. Given the above described role of dopamine and nAChRs in the SNc, and the role of endoplasmic reticulum (ER) stress in PD [28-33], we first summarize the effect of nicotine on expression of dopamine-related, nicotinic receptor, and ER stress-related genes. We find that, broadly speaking, these classes of genes are not significantly altered by chronic nicotine exposure. However, our data reveal that nicotine exposure modulates expression of 129 genes that could be relevant to the neuroprotective effects of smoking including genes involved in (1) the ubiquitin-proteasome pathway, (2) cell cycle regulation, (3) chromatin modification, and (4) DNA binding and RNA regulation. We also report the first draft transcriptome of single-cell dopaminergic and GABAergic neurons isolated from midbrain cultures. Our results give an emerging picture of the role of nicotine on the SNc and on dopaminergic neurons.

2. Materials and methods

2.1 Mice.

All experiments were conducted in accordance with the guidelines for care and use of animals provided by the National Institutes of Health (NIH), and protocols were approved by the Institutional Animal Care and Use Committee at the California Institute of Technology. Mice were kept on a standard 12 h light/dark cycle at 22°C and given food and water ad libitum. On P21, mice were weaned and housed with same-sex littermates.

2.2 Chronic nicotine administration.

Chronic nicotine or saline was administered to C57BL6/DBA mice using mini-osmotic pumps (model 2002; Alzet, Cupertino, CA) for 14 days as described previously [5, 34]. On the day of pump implantation, saline or (−)-nicotine hydrogen tartrate (Sigma, St. Louis) was prepared freshly and loaded into the pump to deliver nicotine at 2 mg/kg/h. This concentration has been shown to provide maximal nAChR upregulation and provides a blood concentration of 590 nM,

which is near the peak concentration in the average smokers' brain [35, 36]. On completion of the 14-day nicotine treatment mice were deeply anesthetized with sodium pentobarbital (100 mg/kg; i.p.) and sacrificed by decapitation. Mice were 4 months of age at the end of chronic nicotine/saline treatment.

2.3 Laser capture microdissection

Our methods pipeline for fabricating cDNA libraries via laser capture microdissection [37-39], and performing RNA-Seq are outlined in Fig. 1. Whole brains from 4 month old male mice (*n=2*) were collected (post-mortem interval of < 5 min), fresh frozen over dry-ice, and stored at -80 °C. Midbrain cryostat sections (20 µm) were mounted on UV-treated Zeiss Membrane Slides (1.0 PEN NF), air dried for 5 minutes, and stained with cresyl violet for 1 minute. The sections were rinsed, dried and then visualized under brightfield illumination at 400X magnification on a Zeiss PALM Laser Capture Micro Dissection microscope. Twenty putative DA^+ cell bodies from the SNc were dissected using multiple low laser energy pulses (see Fig. 2A), and were catapulted into Zeiss 200 µL adhesive caps. Cell lysis solution (Illumina, San Diego, CA) containing 3' SMART reverse transcription primers and quantitation controls ("spikes") were then added into the pool of cells prior to freezing. For comparison we also generated RNA-Seq libraries from 200 pg of untreated mouse whole brain RNA (*n*=2).

2.4 RNA-Seq library generation

To fabricate our cDNA libraries we prepared amplified cDNA from RNA, using Clontech's SMARTer™ Ultra Low RNA system for Illumina Sequencing (Clontech, Mountain View, CA). We used Clontech's Advantage 2 PCR system for the efficient and accurate amplification of cDNA templates by long-distance PCR. Epicentre's Nextera Tn5-mediated tagmentation technology (Epicentre, Madison, WI) was used as an *in vitro* transposition method to simultaneously fragment and tag the cDNA libraries with Illumina compatible sequencing primers. After quality control measures of yield and fragment length distribution were taken using the Qubit fluorometer (Invitrogen, Carlsbad, CA) and the Agilent (Santa Clara, CA) Bioanalyzer, 50 bp or 100 bp sequencing reads were generated on the Illumina HiSeq instrument. Each sequencing library generated > 20 million uniquely mapping reads.

2.5 Computational Analysis

50 bp or 100 bp sequence tags were mapped to the mouse genome using TopHat 1.3.2 [41]. We quantified transcript abundance (FPKM: fragments per kilobase per million mapped reads (expression values)) using Cufflinks. We annotated the transcripts with genome annotations provided by ENSEMBL. We conducted pairwise comparisons and calculated statistical values using Cuffdiff, part of the Cufflinks suite, to identify differentially expressed genes. We assessed ontology with DAVID [42, 43]. Cuffdiff data with FPKM > 1, a corrected *p* value of < 0.05 and a

fold difference of > 1.5 were given as input to Ingenuity Pathway Analysis (IPA) for pathway analysis. Gene expression distribution and scatter plots were generated using the R package cummeRbund [41].

2.6 Immunohistochemistry

Mice (C57BL6) (*n*=3) were deeply anesthetized with sodium pentobarbital (100 mg/kg; i.p.) and perfused transcardially with 15 ml of ice-cold PBS followed by 25 ml of ice-cold 4% paraformaldehyde (PFA) in PBS. Brains were removed and postfixed for 2 h at 4°C with the same fixative and cryoprotected in PBS containing 30% sucrose until the brain sank. Coronal sections (50 µm) were cut on a microslicer and collected into a 12-well tissue culture plate containing PBS. Sections were permeabilized (20 mM HEPES, pH 7.4, 0.5% Triton X-100, 50 mM NaCl, 3 mM $MgCl_2$, 300 mM sucrose) for 1 h at 4 °C followed by blocking (0.1% Triton X-100, 5% donkey serum in TBS) for 1 h at RT. Slices were incubated overnight at 4 °C in solutions containing primary antibodies (diluted in 0.1% Triton X-100, 5% donkey serum in TBS). Primary antibodies and final dilutions were as follows: 1:200 rabbit anti-phospho-eIF2α, (9721, Cell Signaling), 1:500 sheep anti-tyrosine hydroxylase (TH; AB1542, Millipore), 1:250 rabbit anti-XBP1 (sc7160; Santa Cruz), 1:50 rabbit anti-GADD153 (CHOP) (sc575; Santa Cruz Biotechnology). Sections were washed thrice for 10 min each in TBST (0.1% Triton X-100 in TBS) and incubated for 1 h at RT with secondary antibodies (diluted in 0.1% Triton X-100, 5% donkey serum in TBS). Secondary antibodies and final dilutions were as follows: 1:1000 goat anti-rabbit Alexa 488 (A11008; Invitrogen), 1:1000 donkey anti-sheep Alexa 555 (A21436; Invitrogen), 1:1000 donkey anti-mouse Alexa 555 (A31570; Invitrogen), and 1:1000 goat anti-guinea pig Alexa 555 (A21435; Invitrogen). Sections were then washed four times in TBST for 10 min each. All sections were mounted on slides and coverslipped with Vectashield (Vector Laboratories), then imaged with a Nikon Instruments C1 or A1 laser-scanning confocal microscope system equipped with spectral imaging capabilities and a Prior (Rockland) remote-focus device. A Nikon Plan Apo 10X or 60X oil immersion objective was used, and pinhole diameter was 30 µm. Sections were imaged at 12-bit intensity resolution over 512 X 512 pixels at a pixel dwell time of 2– 4 µs. Alexa 488 was excited with an argon laser at 488 nm, and Alexa 555 was excited with a solid-state laser at 561 nm. Imaging was performed using the Nikon DEES grating and spectral detector with 32 parallel photomultiplier tubes. Signals from dyes were unmixed from background autofluorescence similar to our previous studies [44-47].

2.7 Cell culture and single-cell harvesting

To culture primary midbrain neurons from mouse embryos, ventral midbrain tissue from embryonic day 14 embryos was dissected out using standard procedures. Following digestion with papain (15 min at 37 °C), cells were separated by DNAse treatment and trituration, and plated at a density of 100,000 cells per dish in poly-L-ornithine and laminin coated imaging dishes containing Neurobasal medium supplemented with B27, Glutamax, 1% Hyclone equine serum and 100 µm ascorbate. Either control medium (control) or 200 nM nicotine was added to

the culture for two weeks from day 7 to day 21. Media were changed every 3 days. Single cells were harvested on day 21 following a previously reported protocol [48]. Glass capillary tubing (Kimax-51, 1.5-1.8 mm o.d.) was cleaned by sonication in ethanol and then baked overnight at 200°C to inactivate RNAase. Large bore, glass micropipettes (10-30 μm tip diameter) were pulled from the tubing using a Sutter P-50 microelectrode puller. Prior to harvesting, we removed the media from the culture dishes, rinsed them with 2 ml of Dulbecco's PBS, and left 1 ml of Dulbecco's PBS remaining in the dish for harvesting. Individual cultured neurons were identified using a microscope equipped with a 40X phase objective. The pipette was positioned over the cell soma using a motorized micromanipulator (Sutter Instrument Co., USA), the cell was aspirated into the glass micropipette using gentle suction. The micropipette containing the cell was immediately removed from the bathing solution, placed inside a plastic, RNAase-free microcentrifuge tube containing 1.5 μl of RNAase-free PBS and 0.5 μl of an RNAase inhibitor solution, and its tip was broken against the side of the tube near the bottom. We applied outward pressure to the broken micropipette using a large gauge syringe needle to expel the remaining fluid at the tip of the micropipette into the tube. The tube was then centrifuged briefly using a desktop centrifuge and then frozen on dry ice. Typically, 16 cells were harvested per dish over a 1 h period at ambient temperature. The resultant mRNAs were reverse transcribed and amplified to construct single-neuron high-yield cDNA sequencing libraries.

3. Results

3.1 Generation of RNA-Seq libraries from 30 laser captured midbrain cells

Genome-wide transcriptomic analyses are routinely used to monitor specific tissue-, disease-, and cell-type gene expression [49], but it has been technically challenging to generate expression profiles from single cells or from a small number of cells. We first generated RNA-Seq libraries from 30 laser captured midbrain (SNc and VTA) neurons dissected from untreated mouse coronal slices (a representative image for laser capture microdissection is given in (Fig. 2A). Quality control is shown in Fig. 2B, and representative data are shown in Fig. 2C (Libraries 1-3). We obtained > 30 million 50 bp reads, and detected > 10,000 genes, per library, with an excellent distribution of gene expression from 0 to 5000 FPKM. For comparison, we also generated high-quality cDNA libraries from 200 pg of mouse whole brain RNA (*n*=2); representative data are shown in Fig. 2C, Library 4. In addition to sequence-based and quantitative analysis, gene ontology bioinformatics tools were used to analyze these data. The top three gene ontology categories of the 300 most highly expressed genes in midbrain DA^+ neurons were determined using DAVID [42, 43]. The top 3 functional categories of genes are respiratory chain, metabolite/energy and mitochondrion. These functional categories comply with our expectations for dopaminergic neurons.

3.2 Enrichment of nicotinic receptor transcripts in SNc neurons compared to whole brain tissue

We next generated high-quality RNA-Seq libraries from 20 laser captured SNc cells. We conducted Cufflinks and Cuffdiff analysis [41] to compare transcript levels in SNc neurons versus whole brain tissue. Overall 1505 genes had significantly different expression in whole brain (*n=2*) versus SNc libraries (*n=2*); 243 genes had significantly higher expression, and 1262 had significantly lower expression, in SNc neurons as compared to whole brain (with no FPKM threshold applied). The data show that Chrna3, Chrna4, Chrna6, Chrna5, Chrnb2, Chrnb3 and Lynx1 transcripts are present in the SNc neurons. These nAChR genes encode nAChR α3, α4, α6, α5, β2, β3 subunits, respectively, and Lynx1 is a nicotinic receptor modulator. We compared basal transcript levels for nicotinic receptor genes from these laser captured SNc neurons to basal levels in whole brain tissue. Our data show that several nicotinic receptor gene transcripts, namely Chrna4, Chrna6, and Chrnb3, are significantly enriched in SNc cells compared to whole brain tissue (Table 1). Here, Chrna4 and Chrna6 are the most abundantly expressed nicotinic receptor transcripts. We note that that Lynx1 is expressed, but not enriched, in SNc neurons. Other work shows that approximately 90% of SNc neurons are dopaminergic [50], and as expected, our data show an enrichment of tyrosine hydroxylase (TH) transcripts in the SNc neurons compared to whole brain. Tyrosine hydroxylase is enriched 61 fold (42.4 FPKM vs 2588 FPKM). We also measured an enrichment of other dopamine-related genes including Dopa decarboxylase (Ddc) by 84 fold, Slc6a3 (the dopamine transporter DAT) by 207 fold, and Drd2 (the dopamine D2 receptor) by 128 fold (Table 1).

3.3 Transcriptome-wide analysis of SNc neurons after 14 days of exposure to nicotine at 2 mg/kg/h

We assessed gene expression on laser captured SNc neurons from mice treated with either nicotine or saline, to determine the details of gene activation caused by nicotine exposure in this specific neuronal population. We laser captured 20 SNc neurons after 14 days of exposure to nicotine at 2 mg/kg/h (*n=2*), or saline (control) (*n=2*). In order to make a conservative analysis, we applied two criteria. (a) We analyzed data for genes in which both samples (saline and nicotine) show transcripts at a level of > 1 FPKM. (b) We required that Cuffdiff determines a corrected *p* value of < 0.05 for significance between the two samples. With these criteria, which eliminate false positives, we find that a total of 129 genes are modulated, 67 genes are significantly upregulated, and 62 are significantly downregulated, by chronic nicotine exposure.

3.3.1 nAChR subunits

Our study reports the basal transcript expression levels of nAChR α and β subunits and Lynx1 in SNc cells. We investigated the effects of chronic nicotine administration on SNc mRNA levels for nAChR α and β subunits. We detected no significant change in nicotinic receptor transcripts for Chrna4, Chrna6, Chrna3, Chrna5, Chrnb3 and Chrnb2 in nicotine treated versus untreated SNc neurons (Table 2). This result agrees with a previous study [51] suggesting that nicotinic

receptor transcripts are not modulated by nicotine treatment. We also report that Lynx1 is not significantly regulated by chronic nicotine treatment.

3.3.2 Nicotine does not regulate dopamine-related gene transcript levels in wildtype SNc cells.

Animal studies show that the apparent neuroprotective effect of nicotine is at least partially due to nicotine itself [23-27]. We investigated whether chronic nicotine administration could modulate mRNA levels for dopamine-related genes in the SNc. We examined mRNA levels for TH, Ddc, Slc6a3, and Drd2. We found no significant change in dopamine-related transcript levels in nicotine treated versus untreated SNc neurons (Table 2). Hence, nicotine does not regulate gene transcription for dopamine-related genes in wildtype SNc cells.

3.3.3 Nicotine treatment does not modulate the expression of ER stress genes in SNc neurons of wildtype unstressed animals

ER stress markers have been found in human PD postmortem SNc tissue [30]; hence we were interested to test whether nicotine modulates levels of expression of ER stress-associated proteins. We first quantified basal transcript levels for ER stress genes from the laser captured SNc neurons. Table 2 presents novel basal ER stress gene transcript levels for genes from each of the 3 arms of the unfolded protein response (UPR) pathway, in the saline SNc FPKM column. This mRNA result is concordant with our protein study for ER stress genes shown in Fig. 3. We detected protein expression for several ER stress proteins in the SNc of wildtype mice (control). In Fig. 3, protein expression for p-eIF2α, XBP1 and CHOP, each co-stained with TH antibody, are detected in the SNc in wildtype coronal brain sections. Next we examined whether chronic nicotine treatment modulates mRNA expression of ER stress gene in wildtype unstressed SNc neurons. We show that chronic nicotine treatment does not modulate ER stress gene levels in wildtype SNc neurons (Table 2).

3.3.4 SNc neuronal-specific transcript modulations induced by chronic nicotine exposure.

As noted above, we observed 129 SNc neuronal-specific transcript modulations induced by chronic nicotine exposure. Changes in transcript levels for transcription factors, enzymes, transporters and kinase peptidases and nuclear receptors were detected. We next highlight some of these results. Significant changes observed between the control and nicotine treated samples had corrected *p* values that ranged from 0.00 to 0.05, some of which are highlighted below.

Ubiquitin-proteasome pathway. Chronic nicotine exposure significantly upregulates the E2 ubiquitin ligase ubiquitin-conjugating enzyme E2J2 (UBE) by 5.06 fold (corrected *p* value = 0.03). This enzyme is located in the membrane of the endoplasmic reticulum. However, chronic nicotine exposure also significantly decreases the levels of a proteasome subunit and two de-

ubiquitinating enzymes involved in the ubiquitin-proteasome pathway. For example, chronic nicotine significantly decreases the transcript levels of the proteasome (prosome, macropain) activator subunit 2 (PSME2) by 23.27 fold (corrected *p* value = 0.01) and of the ubiquitin specific peptidase 16 (USP16) gene by 26.89 fold (corrected *p* value = 0.026) and the ubiquitinating specific peptidase 34 (USP34) gene by 10.89 fold (corrected *p* value = 0.025). Both latter genes encode de-ubiquitinating (DUB) enzymes.

Cell cycle regulators. Chronic nicotine exposure effects the expression of two cell cycle regulators: it significantly upregulates cell division cycle 26 (CDC26) by 9.93 fold (corrected p value = 0.03) and significantly downregulates cell division cycle 23 (CDC23) by 26.58 fold (corrected *p* value = (0.02). Both CDC proteins have ubiquitin-protein ligase activity.

Chromatin modification. Chronic nicotine exposure significantly upregulates the expression of chromodomain helicase DNA binding protein 4 (CHD4) by 24.4 fold (corrected *p* value = 0.04). CHD4 has DNA methylation and transcriptional repression activity.

DNA binding and regulation of transcription: Zinc finger protein 76 (ZNF76/ Zfp523) and zinc finger with UFM1-specific peptide domain (Zufsp) are both significantly downregulated by nicotine by 43 fold (corrected *p* value = 0.04) and 5.49 fold (corrected *p* value = 0.04) and play a role in DNA binding and regulation of transcription.

RNA processing. Chronic nicotine exposure significantly upregulates the expression of polynucleoide adenyltransferase, poly(A) polymerase alpha (PAPOLA) by 13.1 fold (corrected *p* value = 0.04). It is involved in the processing of RNA and plays a role in cleavage and polyadenylation of pre-mRNA.

3.4 Novel Single-cell DA and GABAergic transcriptomics

We aspirated a single neuron from primary mouse midbrain cultures into a glass pipette made in a patch-clamp pipette puller. The resultant mRNAs were reverse transcribed and amplified to generate a single-neuron, high-yield, good-quality cDNA library. We detected ~5000 genes in the single cell libraries. In our midbrain cultures it was not possible to distinguish visually among GABAergic and dopaminergic neurons. However, the RNA-Seq data show that single-cell transcriptomics unambiguously distinguishes GABAergic from dopaminergic neurons. Discrimination is accomplished by quantifying the mRNA levels of the DA^+ marker gene TH and the GABAergic marker gene Gad1 in the single-cell libraries. To the best of our knowledge this is the first time single cell RNA-Seq libraries have been generated from DA and GABAergic neurons. We present RNA-Seq data for the dopamine-related genes TH, DDC and Slc6a3, and for the GABAergic marker gene Gad1, in two single DA^+ neurons (*n*=1 control media, n=1 nicotine-treated) (Table 3) and in six GABAergic neurons (*n*=4 control media, *n=2* nicotine-treated) (Table 4). We also report the transcript levels of Chrna6 and Chrnb3 and ER stress genes involved in each of the three arms of the UPR in the two single DA^+ neurons and in the six GABAergic neurons. We report Cufflinks FPKM data in Table 3 and Table 4. We observe variability in transcript levels for our genes of interest. We also ran Cuffdiff analysis on the

GABAergic (control) libraries and listed each of the 4 (control) libraries as a biological replicate versus the two nicotine treated cells. The Cuffdiff analysis indicates that nicotine treatment does not regulate ER stress genes. We do not report Cuffdiff analysis on our control versus nicotine-treated dopaminergic neurons as our dopaminergic cell number is too small and we wish to avoid any unwarranted interpretations.

We employ a scatter plot to assess cell heterogeneity between two (control) non-treated GABAergic libraries (Fig. 4A). The GABAergic single cell RNA-Seq data clearly show heterogeneity in expression profiles between single cells of the same type (Fig. 4A). A Pearson's correlation analysis on two control GABAergic cell transcriptomes gives r=0.61 (not shown). We employ distribution plots to compare the expression density/abundance in these two GABAergic cells. For both cells, we observe a broad distribution of transcript expression over 6 orders of magnitude (Fig. 4B).

In summary, we have compiled the first draft transcriptome for dopaminergic and GABAergic neurons isolated from midbrain cultures and the main genes of interest are summarized in Tables 3 and 4. Our future work will further map out single-cell molecular variability (and similarity) associated with cell phenotypes and this will also further highlight cellular pathways that are modulated by nicotine at the single-cell level.

4. Discussion

4.1 We have developed a method for assessing the effects of chronic nicotine exposure on gene expression in SNc neurons. We have successfully combined laser capture microscopy and single cell transcriptomics. We also present initial data from the method.

4.4.1 We observed 129 SNc neuronal-specific transcript modulations induced by chronic nicotine exposure. We discuss the relevance of these findings below.

4.1.2 Nicotine affects transcript levels of ubiquitin-proteasome genes in SNc cells; relevance to Parkinson's disease?

In all tissues, the majority of intracellular proteins are degraded by the ubiquitin–proteasome pathway [52, 53]. The ubiquitin-proteasome pathway contains enzymes (E1, E2 and E3) that link ubiquitin chains onto proteins to mark them for degradation by the 26S proteasome [53]. Here, we show for the first time that nicotine modulates the transcript levels of ubiquitin enzymes and proteasome in SNc neurons. Specifically, we find that an E2 ligase UBE2J2, and a proteasome subunit (PSME2), and two de-ubiquitinating enzymes (USP16 and USP34) are significantly modulated by nicotine exposure. As mentioned earlier mutations in the proteasomal gene UCHL1 (Park 5; proteasomal protein) or in Park2 (Parkin; a ubiquitin E2 ligase) are associated with familial forms of PD. In both sporadic and familial PD, SNc dopaminergic cells

show proteasome dysfunction [54-60]. However, there is an inverse correlation between PD and person's history of smoking. It is not unreasonable to suggest that the modulation of the ubiquitin proteasome pathway may contribute to the putative neuroprotective effects of nicotine and may warrant further investigation.

Previously Kane et al. [61] showed that, after exposure to nicotine for 14 days, ubiquitin enzymes, 20S and 19S proteasomal subunits, and chaperonin-containing complex members are upregulated in 2 mm tissue punches from the rat prefrontal cortex (PFC) and are downregulated in tissue punches taken from the medial basal hypothalamus (MBH). Interestingly, their study makes it clear that ubiquitin-proteasome pathways in different brain regions have different responses to nicotine. However, such regional brain tissue samples are extremely heterogeneous containing hundreds, or perhaps thousands, of cells, with different cell types represented in varying proportions. This makes it challenging to make cell-type specific inferences. We overcame this challenge by conducting RNA-Seq on a small number of cells, from the SNc, dissected from their in situ environment. This allows us to infer that ubiquitin-proteasome transcripts are regulated in dopaminergic neurons of the SNc, a result that may be of relevance to the putative neuroprotective effect of nicotine on the SNc.

In addition to the ubiquitin-proteasome pathway chronic nicotine also significantly modulates other genes that could be relevant to the neuroprotective effects of smoking including genes involved in cell cycle regulation, chromatin modification, and DNA binding and RNA regulation.

4.2 The literature contains many discussions on the relative importance of pulsatile (smoked) vs continued application of nicotine. Our preliminary data cannot settle this point. However we note these arguments for the relevance of continued application: (1) chewed tobacco, which induces brain nicotine levels more slowly than smoking, also has an apparent protective effect, (2) upregulation, the best-studied cellular effect of chronic nicotine exposure, occurs quite robustly with all tested means of nicotine exposure, including smoking, oral administration, and minipumps.

4.3 Chronic nicotine exposure does not regulate nAChR or dopamine-related gene mRNA levels in SNc cells

As discussed earlier, the degeneration of DA neurons in the SNc contributes to the loss of dopamine in the striatum, a brain region involved in the control of movement, leading to diagnostic clinical features of bradykinesia, rigidity and tremor. One protective effect of nicotine may be that nicotine exposure activates SNc nAChRs at the plasma membrane, increasing firing frequency and therefore increasing release of dopamine in the dorsal striatum. Here in this study, we were interested to know if chronic nicotine exposure induces changes in expression levels of nAChR and dopaminergic related genes. Our data show that in SNc cells chronic nicotine exposure does not regulate nAChRs mRNA levels or transcript levels of dopamine-

related genes. These results are concordant with Marks et al. [51]. We also report that the mRNA expression of Lynx1 is not modulated by chronic nicotine exposure.

4.4 Basal levels of ER stress gene transcripts in healthy SNc cells

Nicotine-induced relief of endoplasmic reticulum (ER) stress has been postulated as a potential mechanism for the neuroprotective effects of smoking. Our study assesses whether chronic nicotine significantly affects the expression of ER stress-related genes. Our study reveals the basal level of ER stress gene transcripts in healthy SNc neurons isolated from intact brains. We also find that chronic nicotine exposure does not regulate ER stress gene transcript levels in healthy SNc neurons. However, it is possible that ER stress levels may increase in the SNc of PD brains caused by protein misfolding and high cellular levels of α-synuclein and other PD-related proteins. Indeed higher levels of ER stress markers are seen in PD post mortem studies [30]. The putative neuroprotective effects provided by nicotine may be cumulative over decades and contribute to a prevention of ER stress build-up. If this process occurs, it could contribute to the inverse correlation of PD and a person's history of smoking. Therefore, investigating ER stress gene transcript levels in SNc cells isolated from a PD model that shows dopaminergic cellular dysfunction is warranted.

4.5 Single cell transcriptomics

4.5.1 Single cell transcriptome variability

Recently it has become feasible to measure cell type specific expression [62-64]. Substantial differences in gene expression have been shown for individual cells, even when those cells are taken from a seemingly homogenous population [65-70]. Here we use single cell RNA-seq to investigate the affects of chronic nicotine on GABAergic and dopaminergic neurons isolated from midbrain cultures. We also use this newly developed technique to assess the heterogeneity in neuronal populations. We employ a scatter plot to assess the global similarity and differences between our GABAergic (control) libraries (Fig. 4A). Shalek et al [65] observed that correlation analysis of transcript expression levels between two 10,000–cell population replicates gave r=0.98 showing low heterogeneity. However, gene expression differences between individual cells are averaged out in such bulk preparation comparisons. In contrast a comparison of two single immune cells gave r=0.54, showing high heterogeneity [65]. Here we observe that Pearson's correlation analysis of transcript expression levels of two single GABAergic cells gave r=0.61. Molecular and physiological diversity of midbrain GABAergic neurons has been highlighted by [71]. As discussed in [65], potential influences on single cell heterogeneity include the source of the analyzed cells (*in vitro* versus *ex vivo*), the biological condition of the individual cells, the cellular microenvironment, and of course short bursts of RNA transcription. Variance in gene expression measurements is also influenced by the technical difficulty of capturing minute quantities of mRNA in single cell samples.

4.5.2 Effects of nicotine on ER stress genes in single GABAergic neurons

We find that chronic nicotine exposure does not regulate ER stress gene transcript levels in GABAergic neurons. This result is concordant with our LCM-captured SNc libraries.

4.6 Concluding remarks.

This study highlights the fact that chronic nicotine exposure has a notable effect on the SNc transcriptome, modulating 129 genes and affecting the role of central cellular pathways. These effects may contribute to the putative neuroprotective role of nicotine and may be relevant to PD. More generally, these results reveal the transcriptional effects of nicotine on the brain.

Clinical trials of nicotine patches in early-stage PD have yielded mixed results, and additional trials are under way. We wish to point out the major difference between identifying a target—for instance, nAChRs—and understanding the mechanism. The mechanism includes the very important question of the target's localization (ER vs plasma membrane; see graphical abstract), as the dosing/pharmacokinetic considerations for subcellular action differ greatly from those for plasma membrane action. Specifically, nicotine upregulates nAChRs by pharmacological chaperoning at much lower concentrations than those appropriate for activation. Mechanism also includes the signaling pathways engaged (see graphical abstract); such knowledge will be required both to specify additional drugs that might enhance nicotine neuroprotection, and to design suitable analogs that might be more protective than nicotine itself. Only by understanding mechanistic points will the community be able to leverage the broad hint from nicotine's apparent neuroprotective action.

Acknowledgements

We thank Igor Antoshechkin for library sequencing, sequencing facility management and for computational training, Sheri McKinney for excellent cell cultures and for conducting nicotine administration, and Purnima Deshpande for animal breeding and laboratory management. We thank Prof. John Allman for use of the Zeiss laser capture microscope, Georgi Marinov for some analysis and helpful discussions and Charlotte Yang for initial DAVID analysis. This work was supported by the NIH (DA017279, AG033954), by the California Tobacco-Related Disease Research Program, by the Caltech Innovation Initiative, and by the Millard and Muriel Jacobs Genetics and Genomics Laboratory at California Institute of Technology. We thank the reviewers for helpful and insightful comments.

References

[1] Research for International Tobacco Control. WHO report on the global tobacco epidemic, 2008: the MPOWER package: World Health Organization, 2008.

[2] Barik J, Wonnacott S. Molecular and Cellular Mechanisms of Action of Nicotine in the CNS. In: Henningfield J, London E, Pogun S, editors. Nicotine Psychopharmacology: Springer Berlin Heidelberg, 2009. p. 173-207.

[3] Benowitz NL, Hukkanen J, Jacob P, 3rd. Nicotine chemistry, metabolism, kinetics and biomarkers. Handbook of experimental pharmacology 2009:29-60.

[4] Drenan RM, Nashmi R, Imoukhuede PI, Just H, McKinney S, Lester HA. Subcellular Trafficking, Pentameric Assembly and Subunit Stoichiometry of Neuronal Nicotinic ACh Receptors Containing Fluorescently-Labeled α6 and β3 Subunits. Mol Pharmacol 2008;73:27-41.

[5] Nashmi R, Xiao C, Deshpande P, McKinney S, Grady SR, Whiteaker P, et al. Chronic nicotine cell specifically upregulates functional α4* nicotinic receptors: basis for both tolerance in midbrain and enhanced long-term potentiation in perforant path. The Journal of neuroscience : the official journal of the Society for Neuroscience 2007;27:8202-18.

[6] Nashmi R, Dickinson ME, McKinney S, Jareb M, Labarca C, Fraser SE, et al. Assembly of $\alpha 4\beta 2$ nicotinic acetylcholine receptors assessed with functional fluorescently labeled subunits: effects of localization, trafficking, and nicotine-induced upregulation in clonal mammalian cells and in cultured midbrain neurons. The Journal of neuroscience : the official journal of the Society for Neuroscience 2003;23:11554-67.

[7] Srinivasan R, Pantoja R, Moss FJ, Mackey ED, Son CD, Miwa J, et al. Nicotine up-regulates {alpha}4{beta}2 nicotinic receptors and ER exit sites via stoichiometry-dependent chaperoning. J Gen Physiol 2011;137:59-79.

[8] Tapper AR, McKinney SL, Nashmi R, Schwarz J, Deshpande P, Labarca C, et al. Nicotine activation of α4* receptors: sufficient for reward, tolerance and sensitization. Science (New York, NY) 2004;306:1029-32.

[9] Penton RE, Lester RAJ. Cellular events in nicotine addiction. Seminars in cell & developmental biology 2009;20:418-31.

[10] Albuquerque EX, Pereira EF, Alkondon M, Rogers SW. Mammalian nicotinic acetylcholine receptors: from structure to function. Physiol Rev 2009;89:73-120.

[11] Brunzell DH, Russell DS, Picciotto MR. In vivo nicotine treatment regulates mesocorticolimbic CREB and ERK signaling in C57Bl/6J mice. J Neurochem 2003;84:1431-41.

[12] Brunzell DH, Mineur YS, Neve RL, Picciotto MR. Nucleus accumbens CREB activity is necessary for nicotine conditioned place preference. Neuropsychopharmacology : official publication of the American College of Neuropsychopharmacology 2009;34:1993-2001.

[13] Madsen HB, Brown RM, Lawrence AJ. Neuroplasticity in addiction: cellular and transcriptional perspectives. Front Mol Neurosci 2012;5:99.

[14] Flatscher-Bader T, Wilce PA. The effect of alcohol and nicotine abuse on gene expression in the brain. Nutrition research reviews 2009;22:148-62.

[15] Nestler EJ. Transcriptional mechanisms of addiction: role of ΔFosB. Philosophical Transactions of the Royal Society B: Biological Sciences 2008;363:3245.

[16] Miwa JM, Freedman R, Lester HA. Neural systems governed by nicotinic acetylcholine receptors: emerging hypotheses. Neuron 2011;70:20-33.

[17] Meredith GE, Sonsalla PK, Chesselet M-F. Animal models of Parkinson's disease progression. Acta neuropathologica 2008;115:385-98.

[18] Chesselet M-F, Richter F. Modelling of Parkinson's disease in mice. The Lancet Neurology 2011;10:1108-18.

[19] Nestler EJ, Hyman SE, Malenka RC. Molecular neuropharmacology: a foundation for clinical neuroscience: McGraw-Hill, Medical Pub. Division, 2001.
[20] Ritz B, Ascherio A, Checkoway H, Marder KS, Nelson LM, Rocca WA, et al. Pooled analysis of tobacco use and risk of Parkinson disease. Archives of neurology 2007;64:990-7.
[21] Thacker EL, O'Reilly EJ, Weisskopf MG, Chen H, Schwarzschild MA, McCullough ML, et al. Temporal relationship between cigarette smoking and risk of Parkinson disease. Neurology 2007;68:764-8.
[22] Quik M, Wonnacott S. alpha6beta2* and alpha4beta2* nicotinic acetylcholine receptors as drug targets for Parkinson's disease. Pharmacological reviews 2011;63:938-66.
[23] Quik M, Perez XA, Bordia T. Nicotine as a potential neuroprotective agent for Parkinson's disease. Movement disorders : official journal of the Movement Disorder Society 2012;27:947-57.
[24] Maggio R, Riva M, Vaglini F, Fornai F, Molteni R, Armogida M, et al. Nicotine prevents experimental parkinsonism in rodents and induces striatal increase of neurotrophic factors. Journal of neurochemistry 1998;71:2439-46.
[25] Costa G, Abin-Carriquiry JA, Dajas F. Nicotine prevents striatal dopamine loss produced by 6-hydroxydopamine lesion in the substantia nigra. Brain research 2001;888:336-42.
[26] Ryan RE, Ross SA, Drago J, Loiacono RE. Dose-related neuroprotective effects of chronic nicotine in 6-hydroxydopamine treated rats, and loss of neuroprotection in alpha4 nicotinic receptor subunit knockout mice. British journal of pharmacology 2001;132:1650-6.
[27] Quik M, Parameswaran N, McCallum SE, Bordia T, Bao S, McCormack A, et al. Chronic oral nicotine treatment protects against striatal degeneration in MPTP-treated primates. Journal of neurochemistry 2006;98:1866-75.
[28] Mercado G, Valdes P, Hetz C. An ERcentric view of Parkinson's disease. Trends in molecular medicine 2013;19:165-75.
[29] Lindholm D, Wootz H, Korhonen L. ER stress and neurodegenerative diseases. Cell death and differentiation 2006;13:385-92.
[30] Hoozemans JJ, van Haastert ES, Eikelenboom P, de Vos RA, Rozemuller JM, Scheper W. Activation of the unfolded protein response in Parkinson's disease. Biochemical and biophysical research communications 2007;354:707-11.
[31] Doyle KM, Kennedy D, Gorman AM, Gupta S, Healy SJ, Samali A. Unfolded proteins and endoplasmic reticulum stress in neurodegenerative disorders. Journal of cellular and molecular medicine 2011;15:2025-39.
[32] Stefani IC, Wright D, Polizzi KM, Kontoravdi C. The role of ER stress-induced apoptosis in neurodegeneration. Current Alzheimer research 2012;9:373-87.
[33] Song L, De Sarno P, Jope RS. Central role of glycogen synthase kinase-3beta in endoplasmic reticulum stress-induced caspase-3 activation. The Journal of biological chemistry 2002;277:44701-8.
[34] Xiao C, Nashmi R, McKinney S, Cai H, McIntosh JM, Lester HA. Chronic nicotine selectively enhances α4β2* nicotinic acetylcholine receptors in the nigrostriatal dopamine pathway. The Journal of neuroscience : the official journal of the Society for Neuroscience 2009;29:12428-39.
[35] McCallum SE, Parameswaran N, Bordia T, Fan H, McIntosh JM, Quik M. Differential regulation of mesolimbic $\alpha3^*/\alpha6^*\beta2$ and $\alpha4^*\beta2$ nicotinic acetylcholine receptor sites and function after long-term oral nicotine to monkeys. J Pharmacol Exp Ther 2006;318:381-8.
[36] Marks MJ, Rowell PP, Cao JZ, Grady SR, McCallum SE, Collins AC. Subsets of acetylcholine-stimulated $^{86}[Rb]^+$ efflux and $^{125}[I]$-epibatidine binding sites in C57BL/6 mouse brain are differentially affected by chronic nicotine treatment. Neuropharmacology 2004;46:1141-57.

[37] Boone DR, Sell SL, Hellmich HL. Laser capture microdissection of enriched populations of neurons or single neurons for gene expression analysis after traumatic brain injury. Journal of visualized experiments : JoVE 2013.
[38] Pietersen CY, Lim MP, Macey L, Woo TU, Sonntag KC. Neuronal type-specific gene expression profiling and laser-capture microdissection. Methods in molecular biology (Clifton, NJ) 2011;755:327-43.
[39] Bonaventure P, Guo H, Tian B, Liu X, Bittner A, Roland B, et al. Nuclei and subnuclei gene expression profiling in mammalian brain. Brain research 2002;943:38-47.
[40] Watkins S. Cryosectioning. Current protocols in cytometry / editorial board, J Paul Robinson, managing editor [et al] 2009;Chapter 12:Unit 12 5.
[41] Trapnell C, Roberts A, Goff L, Pertea G, Kim D, Kelley DR, et al. Differential gene and transcript expression analysis of RNA-seq experiments with TopHat and Cufflinks. Nature protocols 2012;7:562-78.
[42] Huang da W, Sherman BT, Lempicki RA. Systematic and integrative analysis of large gene lists using DAVID bioinformatics resources. Nature protocols 2009;4:44-57.
[43] Huang da W, Sherman BT, Lempicki RA. Bioinformatics enrichment tools: paths toward the comprehensive functional analysis of large gene lists. Nucleic acids research 2009;37:1-13.
[44] Mackey ED, Engle SE, Kim MR, O'Neill HC, Wageman CR, Patzlaff NE, et al. alpha6* nicotinic acetylcholine receptor expression and function in a visual salience circuit. The Journal of neuroscience : the official journal of the Society for Neuroscience 2012;32:10226-37.
[45] Briggs CA, Gubbins EJ, Marks MJ, Putman CB, Thimmapaya R, Meyer MD, et al. Untranslated region-dependent exclusive expression of high-sensitivity subforms of alpha4beta2 and alpha3beta2 nicotinic acetylcholine receptors. Molecular pharmacology 2006;70:227-40.
[46] Drenan RM, Grady SR, Whiteaker P, McClure-Begley T, McKinney S, Miwa JM, et al. In vivo activation of midbrain dopamine neurons via sensitized, high-affinity alpha 6 nicotinic acetylcholine receptors. Neuron 2008;60:123-36.
[47] Drenan RM, Nashmi R, Imoukhuede P, Just H, McKinney S, Lester HA. Subcellular trafficking, pentameric assembly, and subunit stoichiometry of neuronal nicotinic acetylcholine receptors containing fluorescently labeled alpha6 and beta3 subunits. Molecular pharmacology 2008;73:27-41.
[48] Morris J, Singh JM, Eberwine JH. Transcriptome analysis of single cells. Journal of visualized experiments : JoVE 2011.
[49] Ramskold D, Luo S, Wang YC, Li R, Deng Q, Faridani OR, et al. Full-length mRNA-Seq from single-cell levels of RNA and individual circulating tumor cells. Nature biotechnology 2012;30:777-82.
[50] Hnasko TS, Hjelmstad GO, Fields HL, Edwards RH. Ventral tegmental area glutamate neurons: electrophysiological properties and projections. The Journal of neuroscience : the official journal of the Society for Neuroscience 2012;32:15076-85.
[51] Marks MJ, Pauly JR, Gross SD, Deneris ES, Hermans-Borgmeyer I, Heinemann SF, et al. Nicotine binding and nicotinic receptor subunit RNA after chronic nicotine treatment. The Journal of neuroscience : the official journal of the Society for Neuroscience 1992;12:2765-84.
[52] Rock KL, Gramm C, Rothstein L, Clark K, Stein R, Dick L, et al. Inhibitors of the proteasome block the degradation of most cell proteins and the generation of peptides presented on MHC class I molecules. Cell 1994;78:761-71.
[53] Lecker SH, Goldberg AL, Mitch WE. Protein degradation by the ubiquitin-proteasome pathway in normal and disease states. Journal of the American Society of Nephrology : JASN 2006;17:1807-19.

[54] Lennox G, Lowe J, Morrell K, Landon M, Mayer RJ. Anti-ubiquitin immunocytochemistry is more sensitive than conventional techniques in the detection of diffuse Lewy body disease. Journal of neurology, neurosurgery, and psychiatry 1989;52:67-71.
[55] Lowe J, McDermott H, Landon M, Mayer RJ, Wilkinson KD. Ubiquitin carboxyl-terminal hydrolase (PGP 9.5) is selectively present in ubiquitinated inclusion bodies characteristic of human neurodegenerative diseases. The Journal of pathology 1990;161:153-60.
[56] Ii K, Ito H, Tanaka K, Hirano A. Immunocytochemical co-localization of the proteasome in ubiquitinated structures in neurodegenerative diseases and the elderly. Journal of neuropathology and experimental neurology 1997;56:125-31.
[57] Auluck PK, Chan HY, Trojanowski JQ, Lee VM, Bonini NM. Chaperone suppression of alpha-synuclein toxicity in a Drosophila model for Parkinson's disease. Science (New York, NY) 2002;295:865-8.
[58] McNaught KS, Belizaire R, Jenner P, Olanow CW, Isacson O. Selective loss of 20S proteasome alpha-subunits in the substantia nigra pars compacta in Parkinson's disease. Neuroscience letters 2002;326:155-8.
[59] Schlossmacher MG, Frosch MP, Gai WP, Medina M, Sharma N, Forno L, et al. Parkin localizes to the Lewy bodies of Parkinson disease and dementia with Lewy bodies. The American journal of pathology 2002;160:1655-67.
[60] Cook C, Stetler C, Petrucelli L. Disruption of protein quality control in Parkinson's disease. Cold Spring Harbor perspectives in medicine 2012;2:a009423.
[61] Kane JK, Konu O, Ma JZ, Li MD. Nicotine coregulates multiple pathways involved in protein modification/degradation in rat brain. Brain research Molecular brain research 2004;132:181-91.
[62] Nelson SB, Hempel C, Sugino K. Probing the transcriptome of neuronal cell types. Current opinion in neurobiology 2006;16:571-6.
[63] Simunovic F, Yi M, Wang Y, Macey L, Brown LT, Krichevsky AM, et al. Gene expression profiling of substantia nigra dopamine neurons: further insights into Parkinson's disease pathology. Brain : a journal of neurology 2009;132:1795-809.
[64] Zheng B, Liao Z, Locascio JJ, Lesniak KA, Roderick SS, Watt ML, et al. PGC-1alpha, a potential therapeutic target for early intervention in Parkinson's disease. Science translational medicine 2010;2:52ra73.
[65] Shalek AK, Satija R, Adiconis X, Gertner RS, Gaublomme JT, Raychowdhury R, et al. Single-cell transcriptomics reveals bimodality in expression and splicing in immune cells. Nature 2013;498:236-40.
[66] Bengtsson M, Stahlberg A, Rorsman P, Kubista M. Gene expression profiling in single cells from the pancreatic islets of Langerhans reveals lognormal distribution of mRNA levels. Genome research 2005;15:1388-92.
[67] Raj A, van Oudenaarden A. Single-molecule approaches to stochastic gene expression. Annual review of biophysics 2009;38:255-70.
[68] Kalisky T, Blainey P, Quake SR. Genomic analysis at the single-cell level. Annual review of genetics 2011;45:431-45.
[69] Feinerman O, Jentsch G, Tkach KE, Coward JW, Hathorn MM, Sneddon MW, et al. Single-cell quantification of IL-2 response by effector and regulatory T cells reveals critical plasticity in immune response. Molecular systems biology 2010;6:437.
[70] Cohen AA, Geva-Zatorsky N, Eden E, Frenkel-Morgenstern M, Issaeva I, Sigal A, et al. Dynamic proteomics of individual cancer cells in response to a drug. Science (New York, NY) 2008;322:1511-6.

[71] Klink R, de Kerchove d'Exaerde A, Zoli M, Changeux JP. Molecular and physiological diversity of nicotinic acetylcholine receptors in the midbrain dopaminergic nuclei. The Journal of neuroscience : the official journal of the Society for Neuroscience 2001;21:1452-63.

Figure 1. Methods pipeline, as performed in our experiments. (1) Dissect out mouse brain, freeze (PMI < 5 minutes). (2) Cryostat section at 20 µm (image [33]). (3) Mount on PEN slide, stain with Cresyl Violet, rinse, (4) Laser capture micro dissection on Zeiss PALM. (5) lyse cells with lysis buffer with dT primer at 72° C. (6) SMART cDNA synthesis; 22 cycles amplification. (7) transposon-mediated "tagmentation" of cDNA. (8) cDNA quality control check and multiplexed sequencing on Illumina HiSeq. (9) Subsequent computational analysis using Tophat, Cufflinks and Cuffdiff [34].

Figure 2. A. Representative image of laser captured SNc neurons, and neurons marked for capture (from a 20 µm coronal section stained with Cresyl violet, scale bar = 80 µm). B. Quality check of cDNA, bioanalyser electropherogram showing that most of the cDNA has length > 700 bp. C. Gene abundance in cDNA libraries from laser-capture microdissection (LCM) of midbrain neurons (SNc and VTA) and whole brain tissue. Libraries #1-3 were each generated from 30 LCM neurons; #4 from whole brain mRNA. These libraries have excellent representation: >10,000 genes are detected at >5 fragments per kilobase of transcript per million fragments sequenced (FPKM). Abundance for the three LCM libraries compares well with whole brain material.

Figure 3. TH immunostaining and ER stress proteins in SNc neurons. Representative images of CHOP, TH, XBP1 and p-eIF2α protein expression in wildtype coronal brain sections are shown. The top panel shows CHOP (red), TH (green) and co-stained (merge) protein expression in SNc neurons (60X, scale bars, 50 µm). The top rightmost image shows CHOP (red) protein expression in the SNc and SNr, (10X, scale bar, 200 µm). The middle horizontal panel shows XBP1 (green), TH (red) and merged protein expression in SNc neurons (60X, scale bar, 50 µm). The lower panel shows p-eIF2α (green), TH (red) and merged protein expression in SNc neurons (60X, scale bars, 50 µm).

Figure 4. Single-cell RNA-Seq analysis of GABAergic neurons. A. Correlation of transcript expression levels between two single GABAergic cells (cell (v) and cell (vi)) reveals substantial transcriptome heterogeneity. B. Distribution plots of gene expression reveal a broad range of expression levels.

Two proposed mechanisms for nicotine-mediated transcriptional regulation

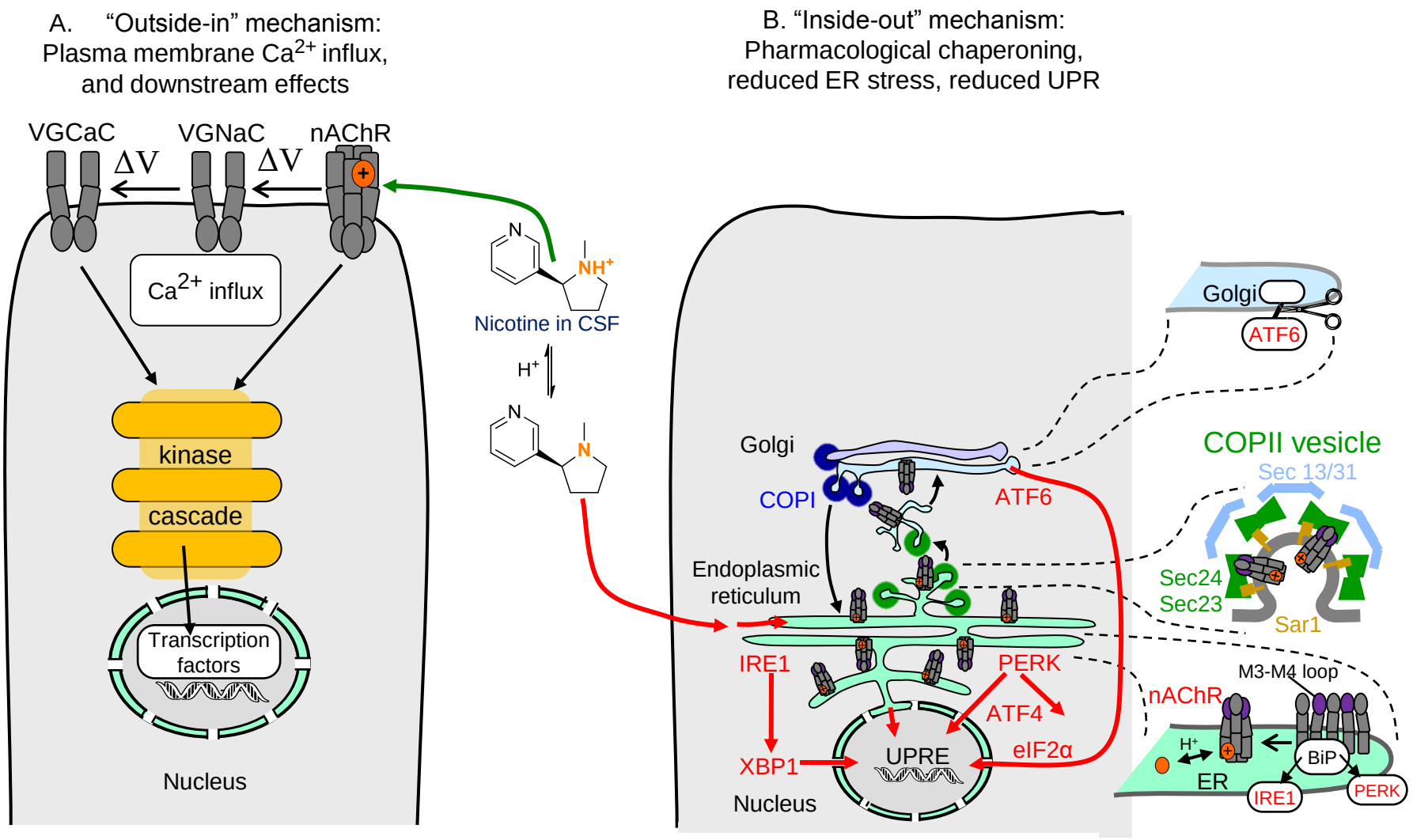

Fig 1 - Henley Lester.pptx

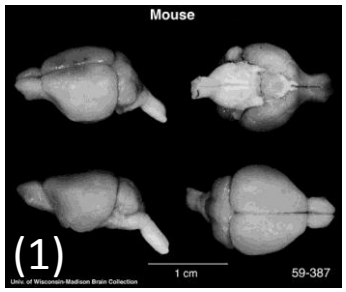

(1)

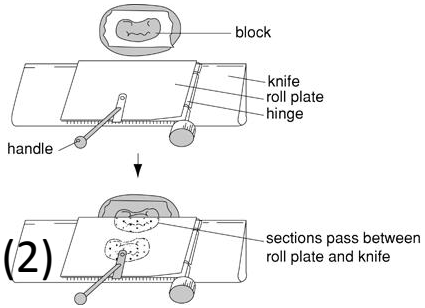

(2)


(3)

(4)


(5)

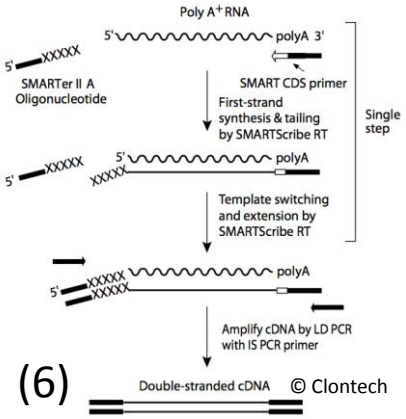

(6) © Clontech

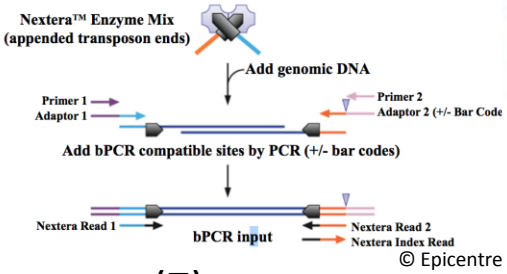

(7) © Epicentre

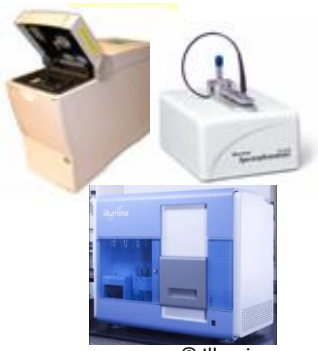
(8) © Illumina

(9)

Bowtie: Fast, general purpose short read aligner

TopHat: aligns RNA-Seq reads to genome; discovers splice sites

Cufflinks / Cuffdiffs: Finds differentially expressed transcripts; detects differential splicing and promoter use

Fig 2 - Henley Lester.pptx

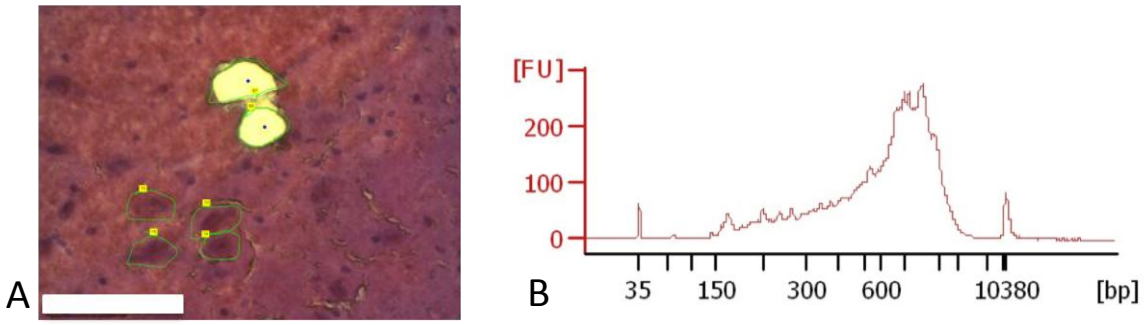

Fig 3 - Henley Lester.pptx

CHOP

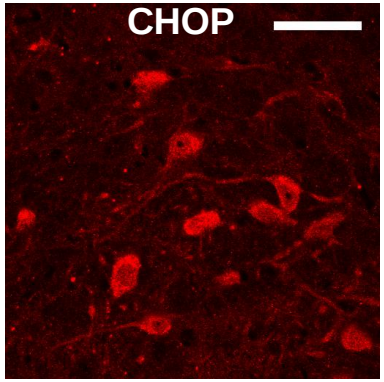

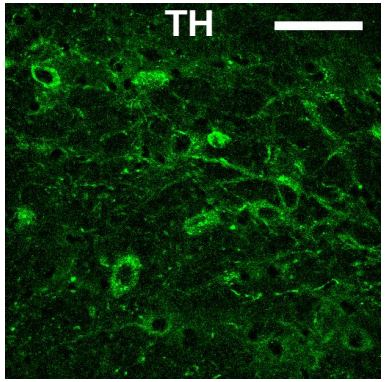

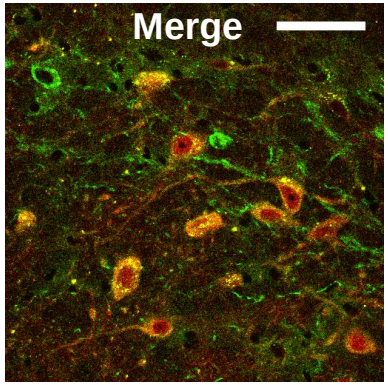

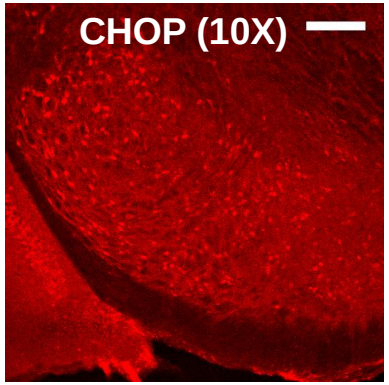

XBP1

(Projections of z stack)

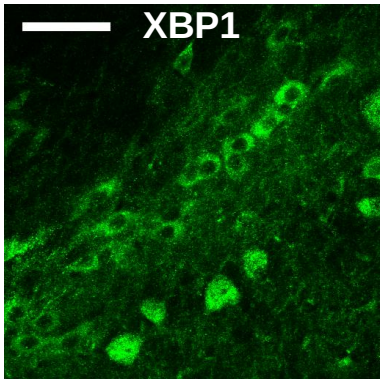

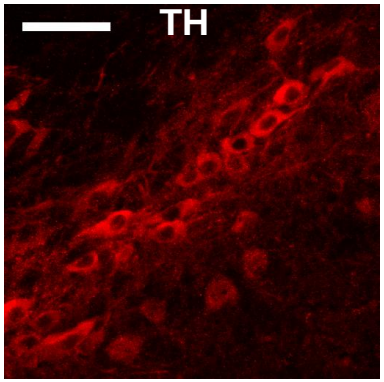

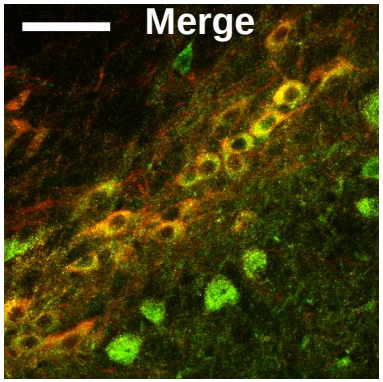

p-eIF2α

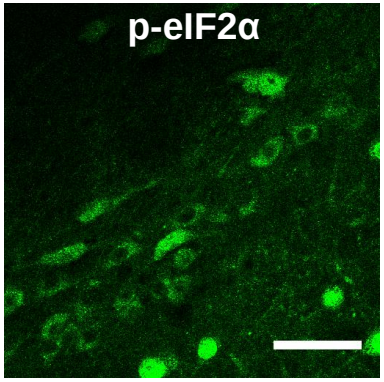

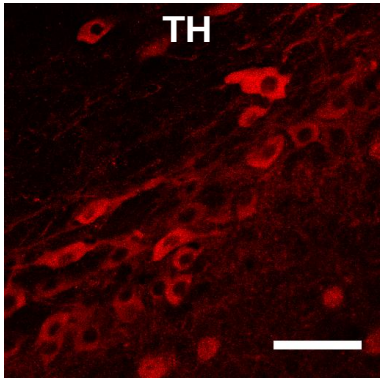

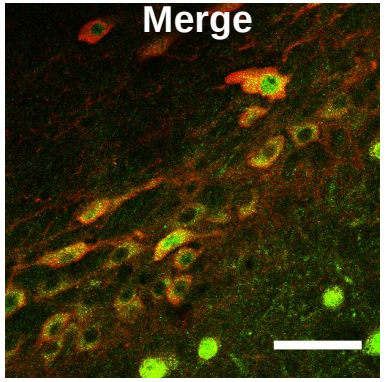

Fig 4 - Henley Lester - resub.pptx